

## Stability of martensitic domains in the ferromagnetic alloy $\text{Ni}_2\text{MnGa}$ : a mechanism for shape memory behaviour

This article has been downloaded from IOPscience. Please scroll down to see the full text article.

2004 J. Phys.: Condens. Matter 16 65

(<http://iopscience.iop.org/0953-8984/16/1/007>)

View [the table of contents for this issue](#), or go to the [journal homepage](#) for more

Download details:

IP Address: 129.252.86.83

The article was downloaded on 27/05/2010 at 12:37

Please note that [terms and conditions apply](#).

# Stability of martensitic domains in the ferromagnetic alloy Ni<sub>2</sub>MnGa: a mechanism for shape memory behaviour

P J Brown<sup>1,2</sup>, B Dennis<sup>2</sup>, J Crangle<sup>2,3</sup>, T Kanomata<sup>2,4</sup>, M Matsumoto<sup>5</sup>,  
K-U Neumann<sup>2</sup>, L M Justham<sup>2</sup> and K R A Ziebeck<sup>2</sup>

<sup>1</sup> Institut Laue-Langevin, BP 156, 38042 Grenoble Cedex 9, France

<sup>2</sup> Department of Physics, Loughborough University, Leicester LE11 3TU, UK

<sup>3</sup> Department of Physics, University of Sheffield, Sheffield S3 7RH, UK

<sup>4</sup> Faculty of Engineering, Tohoku Gakuin University, Tagajo 985, Japan

<sup>5</sup> IMRAM, Tohoku University, TSendai 980-8577, Japan

Received 30 July 2003

Published 15 December 2003

Online at [stacks.iop.org/JPhysCM/16/65](http://stacks.iop.org/JPhysCM/16/65) (DOI: 10.1088/0953-8984/16/1/007)

## Abstract

The martensitic phase transition in Ni<sub>2</sub>MnGa, fundamental to its shape memory behaviour, can be described by two successive 110 type shears leading to 36 possible different orientations for the axes of the pseudo-tetragonal martensitic phase. The distribution and orientation of the domains formed on cooling Ni<sub>2</sub>MnGa into the martensitic phase has been studied using single-crystal neutron diffraction with a multi-detector. The number of domains actually occurring was rather low and was reduced by residual strain. Thermal cycling through the phase transition was found to further reduce the number of domains occurring, which may stabilize after several cycles. Uniaxial stress or a magnetic field applied parallel to [001] is able to switch domains whose pseudo-tetragonal axis is [100] or [010] to ones of type [001]. The results suggest that plastic deformation in the martensitic phase takes place by *twinning* (change of domain), rather than by slip and that the shape memory property arises from the fixed orientation relationship between the martensitic *twins* and the high temperature cubic axes.

## 1. Introduction

Ni<sub>2</sub>MnGa is one of the group of *shape memory effect* alloys which are currently exciting considerable interest. The origin of this effect in Ni<sub>2</sub>MnGa is in the phase change which takes place at  $T_M$  on cooling through 200 K from the cubic  $L2_1$  Heusler structure to a pseudo-tetragonal structure with  $c/a \approx 0.95$ . If the material is plastically deformed in the low temperature martensitic phase and the external load removed it will regain its original shape when heated above the transition temperature. The precise structure of the low

temperature phase depends on both stoichiometry and residual stress; orthorhombic structures with modulations of  $5a/\sqrt{2}$  and  $7a/\sqrt{2}$  have been reported [1]. A recent study showed the structure of an annealed stoichiometric polycrystalline sample to be orthorhombic with  $a_{\text{orth}} = a_{\text{tet}}/\sqrt{2}$ ,  $b_{\text{orth}} = 7a_{\text{tet}}/\sqrt{2}$  and  $c_{\text{orth}} = c_{\text{tet}}$  [2]. The structural transformation can be described in terms of periodic atomic shifts taking place in planes perpendicular to the long  $y$  axis. There is a strong deformation of the cell but only a 1% change in cell volume [3]. This phase transition is remarkable in that, in spite of the strong deformation of the unit cell it is reversible and a single crystal can be cycled through it many times without breaking. The phase transition has been extensively investigated, particularly by inelastic neutron scattering, which reveals the presence of precursor effects above  $T_M$  and an incomplete softening of the TA2 phonon mode at a wavevector  $q$  of 0.33 reciprocal lattice units [4]. A structural modulation with this wavevector, stable below 255 K, leads to the orthorhombic precursor phase with  $a_{\text{orth}} = a_{\text{cub}}/\sqrt{2}$ ,  $b_{\text{orth}} = 3a_{\text{cub}}/\sqrt{2}$  and  $c_{\text{orth}} = c_{\text{cub}}$  [2]. These observations have been correlated with a softening of certain elastic constants [5–7], particularly a 60% reduction in  $c' = (c_{11} - c_{12})$  which is determined by the initial slope of the TA2 phonon propagating in the [110] direction and polarized along [110]. Ultrasonic measurements reveal that the magnitude of  $c'$ , which drives the phase transition, is anomalously low, namely  $0.045 \times 10^{11} \text{ N m}^{-2}$  but the Cauchy pressure ( $c_{12} - c_{44}$ ), which is  $0.4 \times 10^{11} \text{ N m}^{-2}$ , is similar to that observed for pure copper.

Materials exhibiting shape memory effects have potential as actuation devices and smart materials [8]. At 77 K a stress of 2 MPa applied along the [100] direction in  $\text{Ni}_2\text{MnGa}$  has been reported to give rise to a recoverable strain of 5%. Since the compound orders ferromagnetically below  $378 \pm 4 \text{ K}$  the application of a magnetic field can also influence the phase transition. Large strains of nearly 0.2% have been induced along the [100] direction in unstressed crystals of  $\text{Ni}_2\text{MnGa}$  in fields of 0.8 T. This strain is an order of magnitude larger than that which can be induced in the cubic phase and similar to that observed in rare-earth/transition metal compounds, e.g. Terfenol D [9]. The possibility of controlling the shape memory properties by a magnetic field is under active investigation. However, the exact mechanism by which the shape recovery takes place is still not well understood.

A recent [10] determination of the spin density above and below the phase transition suggests that it is driven by a band Jahn–Teller mechanism. Although these measurements revealed the microscopic mechanism giving rise to the phase transition, they shed little light on the processes leading to shape memory. In the present investigation we have tried to address this latter problem by using a multi-detector in conjunction with a four-circle neutron diffractometer to study the distribution and orientation of the pseudo-tetragonal domains which form during the martensitic transformation. The experiments were carried out on annealed and pre-stressed crystals and also on crystals subject to *in situ* stress and applied magnetic fields. Neutron diffraction is a particularly appropriate tool for such a study because the tetragonal distortion is big enough for different domains to be easily resolved both in orientation ( $\omega$ ) and in scattering angle ( $\theta$ ). In addition the low absorption cross-section of the alloy for thermal neutrons allows a relatively large ( $\approx 50 \text{ mm}^3$ ) volume to be sampled.

## 2. Experimental details

### 2.1. Samples

The samples used were six similar pieces  $2 \times 2 \times 5 \text{ mm}^3$  cut from a large single crystal of  $\text{Ni}_2\text{MnGa}$ . The stoichiometry of the crystal was checked by microprobe analysis and was confirmed by the measured martensitic transition temperature of 196 K. For five of them the

long axis was [110] and the two faces of the square cross-section were parallel to (001) and (1 $\bar{1}$ 0). The sixth sample had its longest axis parallel to [001]. In order to check to what extent the behaviour might depend upon annealing, two different treatments were used. Before the experiment the [001] sample and one of the [110] ones were annealed at 800 K and the others at 600 K for 5 days. They were then slowly cooled to room temperature. Their behaviour on thermal cycling through the martensitic transformation was recorded using neutron diffraction. After this first experiment four of the [110] crystals were subjected to 90 GPa at 100 K: for two the pressure was applied parallel to the long axis and for the other two it was along the [001] axis. The thermal cycling experiments were then repeated on the stressed crystals.

## 2.2. Neutron diffraction experiments on annealed and pre-stressed crystals

The neutron diffraction experiments were carried out on the four-circle diffractometer D9 at ILL using a wavelength of 0.84 Å. This diffractometer is equipped with a small multi-detector (32 × 32 pixels) which covers a scattering angle of  $\approx 7^\circ$ . The difference in scattering angle between the  $h00$  and  $00h$  reflections of the pseudo-tetragonal phase is less than  $7^\circ$  for  $h \leq 6$ , so that, if  $h \leq 6$ , all components into which a particular  $\{h00\}$  reflection splits will be recorded by the detector positioned at the scattering angle ( $2\theta$ ) for  $h00$  in the cubic phase. As the crystal, which is undergoing a martensitic transition, is scanned through the reflecting position for a particular  $hkl$ , the detector records the position and intensity of neutrons scattered by the different martensitic variants which grow from the  $hkl$  parent reflection.

For the diffraction experiments the crystals were mounted with their [001] axes approximately parallel to the  $\phi$  axis of the diffractometer. The reflections to be scanned were chosen from the list: 200, 400, 600, 020, 040, 060, 002, 004, 006, 220,  $\bar{2}20$ . The subset of these reflections which could be used in each case was subject to geometrical constraints and to those imposed by the time available for measurement. In all cases at least three perpendicular axial reflections were recorded; for the  $00l$  reflections for which the diffractometer  $\chi \approx 90^\circ$  two perpendicular values of  $\psi$  were chosen so that the corresponding  $\omega$  scans were rotations about [100] and [010], respectively. It was found that a scan over  $10^\circ$  in  $\omega$  was sufficient to record all parts of the reflections. Measurements were made first on cooling from 220 to 174 K and then heating back to 220 K. From 220 to 204 K and from 194 to 174 K the temperature was changed in steps of 4 K; between 204 and 194 K the temperature steps were 2 K. At each step in temperature an  $\omega$  scan of  $10^\circ$ , centred on the position calculated for the cubic phase, was carried out for each reflection in the set. For each sample at least three cooling and two heating cycles were completed.

## 2.3. Neutron diffraction under uniaxial stress

For these experiments the D9 diffractometer was used in its normal beam mode. The [001] axis crystal was mounted on the lower anvil of the pressure cell using silver chloride. It was held in place by lowering the piston by which pressure is applied, until it was just resting on the top surface of the crystal. The crystal and pressure cell were placed in an ILL ‘orange’ cryostat and the crystal was cooled to the martensitic phase in this state (nominally zero stress). It was found that essentially no domains with their (short)  $c$  axis parallel to [001] were present at low temperature. Loads of up to 200 MPa applied in the martensitic phase at 5 K had no measurable effect on either the domain distribution or the mosaic width of the reflections. Above 300 MPa there was a significant increase in the peak widths, which was primarily elastic, as the mosaic returned to almost its original width when the pressure was removed. The scans through the 040 reflection for different values of applied stress are shown in figure 1. It was estimated that

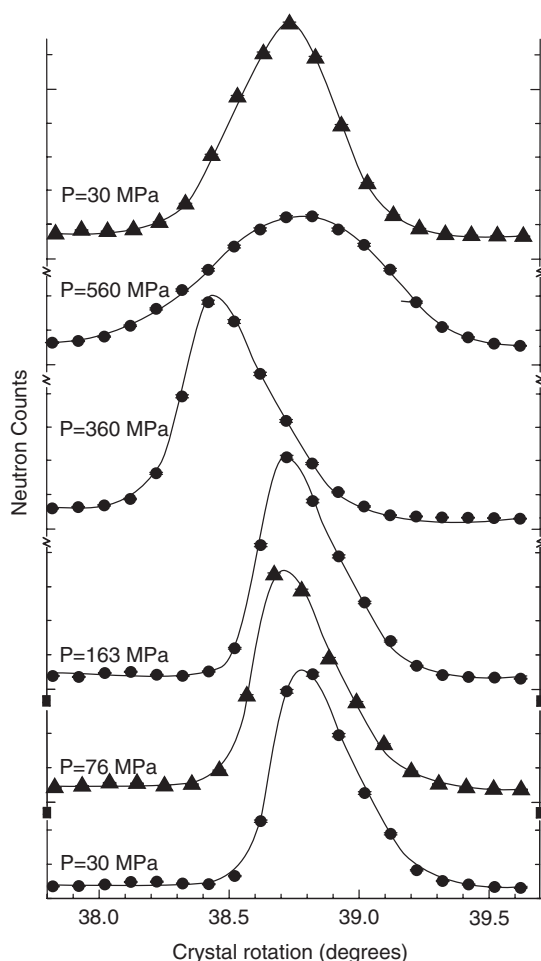


**Figure 1.** Intensity recorded as a function of the crystal rotation  $\omega$  at 5 K in scans through the position of the cubic 040 reflection for different values of applied stress. The scan shown at the top of the figure (triangular markers) was obtained after removing the 600 MPa load.

the holding force of the upper piston was equivalent to  $\approx 30$  MPa; so, to determine whether this small stress was influencing the domain distribution, a second cooling cycle was carried out with the crystal just supported on the lower anvil. In the martensitic phase, domains with all three  $\langle 001 \rangle$  axes as pseudo-tetragonal  $c$  axes were present, the major component having  $c \parallel [100]$ . Lowering the piston onto the sample at 172 K produced a dramatic effect; the  $[100]$  domain disappeared, being replaced by a single  $[001]$  type. This new domain distribution could not be changed by raising the piston to remove the stress. Only after heating the crystal above the martensitic transition and recooling were  $[010]$  and  $[100]$  type domains restored. This behaviour is illustrated in figure 2 which shows the integrated detector counts as a function of scattering angle ( $2\theta$ ) for the 400 reflection.

#### 2.4. Neutron diffraction under magnetic field

The effect of magnetic field on the domain distribution in the martensitic phase was studied using the single-crystal diffractometer D10 at the ILL in normal beam mode. The wavelength

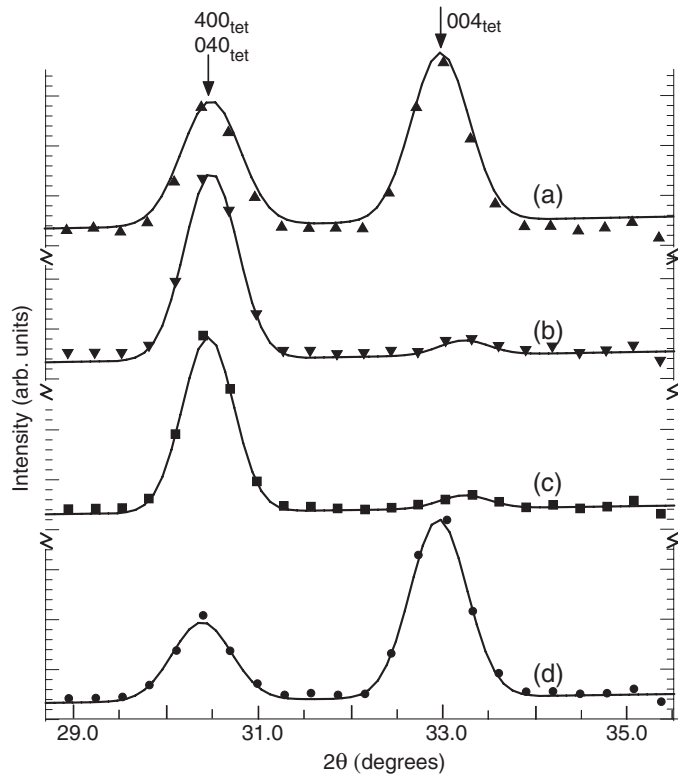


**Figure 2.** Intensity recorded at 172 K in scans through the position of the cubic 400 reflection plotted against the scattering angle ( $2\theta$ ). (a) After cooling with no applied stress, (b) is (a) with 30 MPa applied at 172 K  $\parallel$  [001]; (c) is (b) with the 30 MPa stress removed and (d) is after heating to 250 K and recooling with no stress applied. The higher angle peak in the scans is due to domains with the pseudo-tetragonal  $c$  axis parallel to  $[100]_{\text{cubic}}$ ; they are suppressed by applying the stress.

used was 1.26 Å and the neutrons were recorded with a  $32 \times 32$  pixel multi-detector. The [001] axis crystal was mounted with its long axis parallel to the field direction of a vertical field superconducting magnet. The crystal was cooled in zero field to the martensitic phase ( $T \approx 180$  K); an  $\omega$  scan around the position of the cubic 200 reflection clearly revealed scattered intensity from the 200 and 002 reflections of tetragonal domains with both  $a$  and  $c$  axes nearly parallel to the original cubic  $\langle 100 \rangle$  directions (figure 3(a)). The application of a very small field between 0.02 and 0.03 T gave the same result as applying a uniaxial stress: the domains with  $c$  axes parallel to  $[100]$  and  $[010]$  practically disappeared whilst those with their  $c$  axes parallel to the field direction grew (figure 3(b)). Further increase of the field in steps to 2 T had only a small effect. The mosaic width at both the 200 and 020 reflection positions gradually decreased, suggesting that at high fields a single orthorhombic orientation was favoured. This was confirmed by measurement at 2 T of the intensities of reflections with indices  $h \pm \frac{3}{7}, k \pm \frac{3}{7}, l$  with respect to the pseudo-tetragonal axes. Those corresponding to the modulation  $(\frac{3}{7}\frac{3}{7}0)$  were found to be much stronger than those for  $(\frac{3}{7}\frac{3}{7}0)$ . In terms of the orthorhombic cell the favoured domain is that with the long  $b$  axis nearly parallel to  $[110]_{\text{cubic}}$ .

Fields of up to 2 T were found to have no effect either on the stability ranges or on the lattice parameters of the two orthorhombic phases. Nor was there any significant change with field of the relative intensities of satellite reflections belonging to the same domain in either the

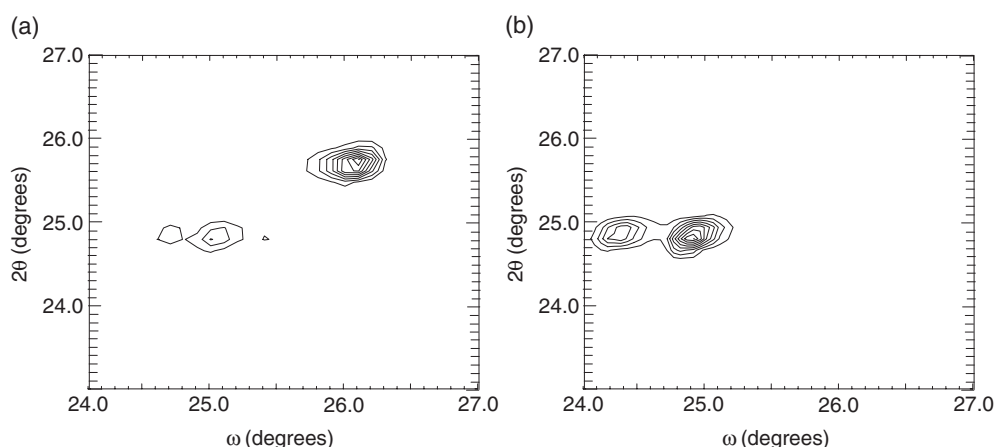


**Figure 3.** Contour plots showing the distribution of scattered intensity in scans through the position of the cubic 200 reflection of  $\text{Ni}_2\text{MnGa}$  at 180 K. (a) In zero field. (b) With 0.03 T applied parallel to [001]. The intensity at the higher  $2\theta$  value is scattered by domains for which the pseudo-tetragonal  $c$  axis is parallel to [100] and that at lower  $2\theta$  by those for which it is parallel to [010] or [001].

precursor (1/3) or martensitic (1/7) phases. This shows that, although applying a magnetic field has a profound effect on the populations of the martensitic domains it has a negligible effect on the structure of the domains themselves.

### 3. Analysis of the results

A preliminary analysis of the data was made by preparing a contour plot for each scan to show the variation in the course of the scan of the recorded count, summed over the vertical pixels of the detector. The horizontal axis of the plot corresponds to successive steps in crystal rotation ( $\omega$ ) and the vertical axis to the horizontal pixel number ( $X$ ) of the detector; lower values of  $X$  correspond to higher scattering angles ( $2\theta$ ). Figure 4 shows example plots of the 400 and 040 reflections from an annealed sample above, during and below the transition.

The qualitative conclusions that could be drawn were: firstly that at temperatures above 206 K all the samples resume their original form, giving, in each thermal cycle, a single well-formed diffraction peak in a constant position no matter how many different peaks were present in the martensitic phase. Secondly the experiments on the annealed and pre-stressed crystals showed that the number and orientation of the martensite domains observed in the transformed phase is different for each sample; it evolves during thermal cycling, becoming generally simpler and stabilizing after several cycles. The number of different domains which were formed on first cooling was significantly larger for the annealed crystals than for the stressed ones. The temperature range within which the martensite domains form and grow (or shrink) is 200–196 K on cooling and 198–202 K on warming; the same for both annealed and stressed samples. The experiments under external constraint showed that the domain structure can be profoundly modified by very small values of either uniaxial stress or magnetic field applied either during cooling or in the martensitic phase. Uniaxial stress, or magnetic field applied parallel to the cubic [001] axis, was able to switch domains whose pseudo-tetragonal  $c$  axis was parallel to cubic [100] or [010] to ones in which it was parallel to the field direction.

A more quantitative analysis of the data was attempted by using the 'PREWASH' program [11]. This program searches for peaks in a multi-detector scan which satisfy chosen criteria. A peak must include pixels for which the recorded count is greater than a chosen

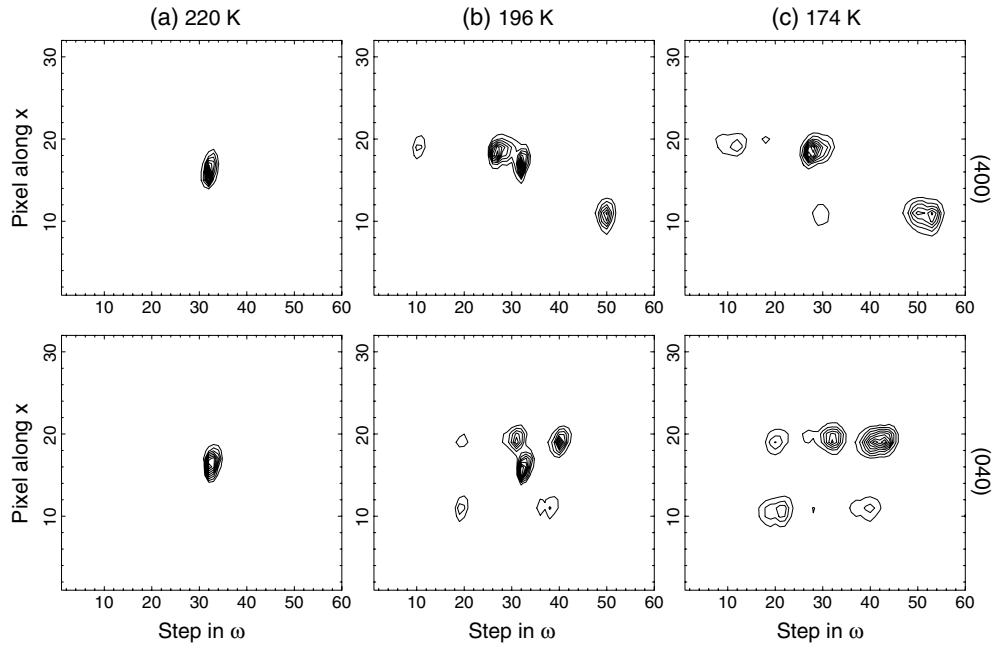


**Figure 4.** Contour plots of the counts summed over the vertical pixels of the detector from 7 to 25 as a function of the scattering angle (vertical axis) and the scan step (horizontal axis) for scans through the 040 and 400 reflections of an annealed crystal. Higher values of  $X$  correspond to smaller scattering angles. At 220 K (a) the sample is in the cubic phase, at 196 K (b) it is transforming and at 174 K (c) it is in the pseudo-tetragonal phase.

multiple of the mean count per pixel; in addition, these pixels must be correlated over a chosen minimum number of consecutive frames. Having identified a peak, the program calculates the position of its centre, its approximate integrated intensity and the orientation and extent of its ellipsoidal shape. For the present data a peak-to-background ratio of 50 correlated over 4 frames ( $\approx 0.4^\circ$ ) enabled all the peaks appearing in the contour plots to be found. Since there is no significant evolution in the domain patterns between 194 K and the lowest temperature of the cycles, only the scans recorded before first cooling and at the lowest temperatures of each cycle were treated at this point.

From the results of 'PREWASH' it was possible, in most cases, to identify those peaks corresponding to the same pseudo-tetragonal domain in the scans of different reflections. This process was quite difficult until it was recognized that there was a high probability of twinning about a common  $a$  axis: the corresponding  $\{h00\}$  reflections to which all twin components contribute were consequently anomalously strong. The positions of the peaks belonging each domain which could be uniquely identified were grouped together and used to determine the matrix describing the pseudo-tetragonal reciprocal axes in terms of the cubic ones. A 'quality' factor, proportional to the non-orthogonality of the resulting matrix was calculated in each case; this allowed peaks which had been improperly assigned to particular domains to be identified.

As a result of this analysis it was found that all significant peaks in the low temperature scans could be assigned to pseudo-tetragonal domains with essentially the same lattice parameters ( $a = 5.915(3)$ ,  $c = 5.571(4)$ ). It was notable that, for the stressed samples, the population of domains with the pseudo-tetragonal  $c$  axis parallel to  $[001]$  was higher than expected (60%) after the first cooling and lower than expected (essentially zero) after several



thermal cycles. In the annealed samples the initial population was 33%, which dropped to 13% after thermal cycling. It was also noticed that the absolute values of those off-diagonal elements of the transformation matrices which describe rotations about the pseudo-tetragonal  $c$  axis tended to be smaller than those giving rotations about the  $a$  axes.

#### 4. General transformation due to two successive shear distortions

A general shear stress, such as those expected to occur in martensitic transformations, can be described by a shear displacement  $\tau$  in a plane  $\mathbf{k}$ ;  $\tau$  must lie in the plane so  $\tau \cdot \mathbf{k} = 0$ . The displacement of a point with radius vector  $\mathbf{r}$  due to this stress is

$$\delta = (\mathbf{r} \cdot \mathbf{k})\tau \quad (1)$$

and the matrix  $\mathbf{M}$  describing the transformation of the unit cell  $\mathbf{r}' = \mathbf{M} \mathbf{r}$  is given by

$$M_{ij} = \delta(ij) + \tau_i k_j. \quad (2)$$

For two successive shears  $\tau$  on  $\mathbf{k}$  and  $\sigma$  on  $\mathbf{q}$ , small enough for the products of the displacements to be negligible, the matrix, written out in full, becomes

$$\mathbf{M} = \begin{pmatrix} 1 + \tau_1 k_1 + \sigma_1 q_1 & \tau_1 k_2 + \sigma_1 q_2 & \tau_1 k_3 + \sigma_1 q_3 \\ \tau_2 k_1 + \sigma_2 q_1 & 1 + \tau_2 k_2 + \sigma_2 q_2 & \tau_2 k_3 + \sigma_2 q_3 \\ \tau_3 k_1 + \sigma_3 q_1 & \tau_3 k_2 + \sigma_3 q_2 & 1 + \tau_3 k_3 + \sigma_3 q_3 \end{pmatrix}. \quad (3)$$

The matrix represents an orthogonal transformation if

$$\begin{aligned} \tau_1 k_2 + \tau_2 k_1 &= -\sigma_1 q_2 - \sigma_2 q_1 \\ \tau_2 k_3 + \tau_3 k_2 &= -\sigma_2 q_3 - \sigma_3 q_2 \\ \tau_3 k_1 + \tau_1 k_3 &= -\sigma_3 q_1 - \sigma_1 q_3 \end{aligned} \quad (4)$$

and in this case the volume of the transformed cell, given by

$$V' = V(1 + \tau_1 k_1 + \sigma_1 q_1 + \tau_2 k_2 + \sigma_2 q_2 + \tau_3 k_3 + \sigma_3 q_3), \quad (5)$$

is unchanged because of the orthogonality between  $\tau$  and  $\mathbf{k}$ , and  $\sigma$  and  $\mathbf{q}$ .

#### 5. Martensitic twinning in Ni<sub>2</sub>MnGa

In Ni<sub>2</sub>MnGa the shears are expected to be on the 110 planes in the  $(\bar{1}10)$  directions. Taking  $\mathbf{k}$ ,  $\tau$  as (011),  $[0\bar{1}\tau]$  and  $\mathbf{q}$ ,  $\sigma$  as (101)  $[\sigma 0\bar{\sigma}]$ ; the transformation matrix becomes

$$\mathbf{M} = \begin{pmatrix} 1 + \sigma & 0 & \sigma \\ 0 & 1 - \tau & -\tau \\ -\sigma & -\tau & 1 + \tau - \sigma \end{pmatrix}. \quad (6)$$

For the pseudo-tetragonal martensitic phase of Ni<sub>2</sub>MnGa  $c/a < 1$ , so either  $\tau = -\sigma$  and the  $c$  axis of the pseudo-tetragonal cell is parallel to the cubic [001] direction, or  $\tau = 2\sigma$  and the  $c$  axis is parallel to [010]. These two possibilities are described by the matrices

$$\mathbf{M}_{1xy} = \begin{pmatrix} 1 + \sigma & 0 & \sigma \\ 0 & 1 + \sigma & \sigma \\ -\sigma & -\sigma & 1 - 2\sigma \end{pmatrix} \quad \mathbf{M}_{2xy} = \begin{pmatrix} 1 + \sigma & 0 & \sigma \\ 0 & 1 - 2\sigma & -2\sigma \\ -\sigma & 2\sigma & 1 + \sigma \end{pmatrix}. \quad (7)$$

The first subscript in the label of a matrix indicates whether it arises from equal shears (type 1) or if the second shear is twice the first (type 2). The second and third subscripts indicate the axial direction perpendicular to the first and second shear planes, respectively. The type 2 matrices correspond to the transformation used by [12] to describe the structural phase transition in

V<sub>3</sub>Si. Although the tetragonal cells generated by the two types of shear are congruent, their orientations with respect to the original unit cell are quite different. A tetragonal cell with  $c$  axis nearly parallel to the cubic [001] axis can arise from type 1 shears on (011) and (101) as above, or from type 2 shears of either:  $\sigma$  on (110) and  $2\sigma$  on (101) or  $-\sigma$  on (110) and  $-2\sigma$  on (011). The matrices corresponding to the latter two are

$$\mathbf{M}_{2zy} = \begin{pmatrix} 1 + \sigma & -\sigma & -2\sigma \\ \sigma & 1 + \sigma & 0 \\ -2\sigma & 0 & 1 - 2\sigma \end{pmatrix} \quad \mathbf{M}_{2zx} = \begin{pmatrix} 1 + \sigma & \sigma & 0 \\ -\sigma & 1 + \sigma & 2\sigma \\ 0 & -2\sigma & 1 - 2\sigma \end{pmatrix}. \quad (8)$$

The three matrices,  $\mathbf{M}_{1xy}$ ,  $\mathbf{M}_{2zy}$  and  $\mathbf{M}_{2zx}$ , have identical diagonal components but are distinguished by their off-diagonal terms which describe the orientation of the tetragonal axes with respect to the cubic ones; for example, the component  $M_{23}$  gives the rotation of the  $y$  and  $z$  axes about  $x$ . In all three matrices one of the three pairs of off-diagonal elements is zero and this may be used to identify the shears, giving rise to different domains in the transformed crystal. For the type 1 domains it is the tetragonal  $c$  axis about which there is no rotation, whereas for type 2 domains it is one or other of the  $a$  axes. The shear displacement  $\sigma = 2(a - c)/3(a + c)$ . For type 1 shears the mean rotation about the three axes is  $2\sigma/3$  whereas for type 2 it is  $\sigma$ .

The two shears giving rise to the type 1 matrices are equivalent: there are 12 different ways in which pairs of {110} planes inclined at 120° to one another may be chosen, leading to 12 differently oriented type 1 twin domains. Each type 1 twin shares one  $a$  axis with another twin and the other  $a$  axis with a third. For type 2 matrices the two shears are distinct, so there are 24 differently oriented type 2 twin domains. Each type 2 twin shares its  $c$  axis with one other member of the set and one of its  $a$  axes with a third.

### 5.1. Comparison with experiment

The precision with which the rotation matrices could be determined was not very good and the values obtained for the small off-diagonal elements were often not much bigger than their uncertainties. These elements were therefore treated statistically rather than individually. For the majority of the domains observed in all the experiments the orientation of the pseudo-tetragonal axes with respect to the cubic ones indicate only a small rotation of the  $x$  and  $y$  pseudo-tetragonal axes about  $z$  with larger rotations about  $x$  and  $y$ . This is the behaviour typical of the type 1 domains defined above. To obtain a more quantitative assessment the domains identified in 3 were classified as type 1 or 2 according to which of the pairs of off-diagonal components had the smallest absolute value. It was found that type 1 domains occurred with more than twice the frequency of type 2 amongst both the annealed and the stressed samples. Using this classification, the mean rotations for the two types of domains were calculated. These gave  $\sigma = 0.019(3)$  for the type 1 domains and  $\sigma = 0.14(2)$ ,  $2\sigma = 0.24(2)$  for the type 2 domains. The value calculated from the lattice parameters is  $\sigma = 0.020$ . The rotations are thus roughly in accord with the model for the type 1 domains but are significantly smaller than expected for the type 2 domains.

In a few cases the positions of superstructure reflections belonging to the low temperature orthorhombic phase were measured. This allowed the orientation of the long orthorhombic  $y$  axis with respect to the rotation matrices to be determined. For all five type 1 domains for which data were available this axis was found to be parallel to the bisector of the normals to the two slip planes involved. For type 2 domains the long  $y$  axis is either parallel or perpendicular to the slip plane on which the smaller of the two shears occurs. These two directions each occurred twice in the four domains studied.

## 6. Discussion

The results of these experiments show that there are well defined relationships between the orientation of the twin domains which are present in the martensitic phase and the original cubic axes. These relationships are largely consistent with the model in which the transition takes place by two successive shears on  $110$  planes in  $\langle 110 \rangle$  directions. The occurrence of domains (type 1) obtained from two equivalent shears is more than twice as probable as those (type 2) in which one shear has twice the magnitude of the other. On heating the same shears take place but in the reverse directions so that a crystal always resumes its original orientation in the cubic phase. There are 36 different ways in which the two shears can be chosen to give a pseudo-tetragonal transformed cell. These would give rise to 36 differently oriented twin domains. It was found, however, that the number of domains which are actually present in transformed single crystals was much less than this with two or three usually being predominant. This paucity of domains is probably due to the persistence of residual stress. The number of domains formed in the pre-stressed crystals was significantly less than in the annealed ones and the presence of even a small applied stress had a profound effect on the domain populations.

These results also suggest that it is magnetostrictive strain rather than crystalline anisotropy which is responsible for the change in domains brought about by applying a magnetic field. The orientation of the  $[100]$  and  $[010]$  type domains which form on application of a field (figure 3(b)) is the same as that of those already present, though in smaller numbers (figure 3(a)). This makes it seem likely that the domains change identity by simple reversal of the unfavourable shears. For example, a  $[010]$  domain formed by type 1 shears on  $101$  and  $011$  will change to an  $[001]$  domain of type 2 if the shear on  $011$  is reversed and doubled. Similarly a  $[100]$  domain of type 2 formed by shears on  $110$  and  $101$  can be converted to a type 1  $[001]$  domain by reversing and halving the shear on  $101$ .

The foregoing observations provide some very strong pointers to the mesoscopic origin of the shape memory effect. We have shown that very small amounts of stress applied in the martensitic phase introduce an inelastic response in the martensitic domain populations. It is suggested that such stress-induced twinning substitutes for normal slip, by movement of dislocations, in the plastic deformation process. The martensitic twin domains transform into one another, those whose  $c$  axes are parallel to the axis of stress being favoured. However, the class of domains which can form is restricted to those which bear fixed relationships to the parent cubic crystal. These relationships being constrained by the orientation of the  $\{110\}$  planes on which the shears, which give rise to the transformation, occur. When the reverse shears occur on warming, they all lead to the original cubic orientation. A polycrystalline sample in the martensitic phase would consist of a large number of different martensitic twin domains, each of which would have formed part of a parent cubic crystallite with a certain orientation. Deformation in the martensitic phase would have the same effect within the crystallite as applying stress to the single crystal; the crystallite would deform plastically due to irreversible changes in the domain populations. However, all the domains formed from a single cubic crystallite always transform back into the original orientation regardless of how their populations may have been changed in the martensitic phase. Hence the original shape is restored.

## 7. Conclusions

The orientation relationships between the axes of the cubic and martensitic phases of  $\text{Ni}_2\text{MnGa}$  allow the shears giving rise to the phase transition to be identified. The seven-fold orthorhombic

structure of this latter phase has been confirmed. Inelastic strains in the transformed phase were shown to be accommodated by twinning, resulting in changes in domain populations, rather than by slip. It is the disappearance of these domains on heating above the phase transition which enables the strains to be reversed. Thus the mesoscopic origin of shape memory behaviour resides in the fixed orientation relationships between the martensitic twins and the crystallographic axes of the high temperature parent phase.

### Acknowledgments

The authors would like to thank J Archer, J-P Laborier, R Note and S Pujol for their excellent technical support.

### References

- [1] Martynov V V and Kokorin V V 1992 *J. Physique* III **2** 739
- [2] Brown P J, Crangle J, Kanomata T, Matsumoto M, Neumann K-U, Ouladdiaf B and Ziebeck K R A 2002 *J. Phys.: Condens. Matter* **14** 10159
- [3] Webster P J, Ziebeck K R A, Town S L and Peak M S 1984 *Phil. Mag.* B **49** 295
- [4] Zheludev A, Shapiro S M, Wochner P, Schwartz P, Wall M and Tanner L E 1995 *Phys. Rev. B* **51** 11310
- [5] Manosa L, Gonzalez-Comas E, Obrado E, Planes A, Cherenko V A, Korkin V V and Cesari E 1997 *Phys. Rev. B* **55** 11068
- [6] Planes A, Obrado E, Gonzalez-Comas E and Manosa L 1997 *Phys. Rev. Lett.* **79** 3926
- [7] Obrado E, Gonzalez-Comas E, Manosa L and Planes A 1998 *J. Appl. Phys.* **83** 7300
- [8] O'Handley R C 1998 *J. Appl. Phys.* **83** 3263
- [9] Murray S J, Farinelli M, Kantner C, Huang J K, Allen S M and O'Handley R C 1998 *J. Appl. Phys.* **83** 7297
- [10] Brown P J, Bargawi A Y, Crangle J, Neumann K-U and Ziebeck K R A 1999 *J. Phys.: Condens. Matter* **11** 4715
- [11] Wilkinson C and Khamis H 1982 *AIP Conf. Ser.* **89** 111
- [12] Batterman B W and Barret C S 1964 *Phys. Rev. Lett.* **13** 390